AIP | Applied Physics Letters

Semiconductor nanowires for highly sensitive, room-temperature detection of terahertz quantum cascade laser emission

Miriam S. Vitiello, Leonardo Viti, Lorenzo Romeo, Daniele Ercolani, G. Scalari et al.

Citation: Appl. Phys. Lett. **100**, 241101 (2012); doi: 10.1063/1.4724309
View online: http://dx.doi.org/10.1063/1.4724309
View Table of Contents: http://apl.aip.org/resource/1/APPLAB/v100/i24
Published by the AIP Publishing LLC.

Semiconductor nanowires for highly sensitive, room-temperature detection of terahertz quantum cascade laser emission

Miriam S. Vitiello,[1] Leonardo Viti,[1] Lorenzo Romeo,[1] Daniele Ercolani,[1] G. Scalari,[2] J. Faist,[2] F. Beltram,[1] L. Sorba,[1] and A. Tredicucci[1]
[1]*NEST, Istituto Nanoscienze–CNR and Scuola Normale Superiore, Piazza San Silvestro 12, Pisa I-56127, Italy*
[2]*Zurich Physics Department, Institute of Quantum Electronics, ETH Hönggerberg, HPT H 6 Wolfgang-Pauli-Str. 16, CH-8093 Zürich, Switzerland*

(Received 28 February 2012; accepted 9 April 2012; published online 11 June 2012)

We report on the development of nanowire-based field-effect transistors operating as high sensitivity terahertz (THz) detectors. By feeding the 1.5 THz radiation field of a quantum cascade laser (QCL) at the gate-source electrodes with a wide band dipole antenna, we record a photovoltage signal corresponding to responsivity values >10 V/W, with impressive noise equivalent power levels $<6\times10^{-11}$ W/$\sqrt{}$Hz at room temperature and a wide modulation bandwidth. The potential scalability to even higher frequencies and the technological feasibility of realizing multi-pixel arrays coupled with QCL sources make the proposed technology highly competitive for a future generation of THz detection systems. © *2012 American Institute of Physics*. [http://dx.doi.org/10.1063/1.4724309]

Terahertz (THz) technology has become of large interest over the last few years for its potential in non-invasive imaging applications spanning from medical diagnostics to homeland security[1] as well as for its peculiar sensitivity to many molecular absorption lines, appealing for spectroscopic[2] and biological analysis.[3] In this context, the development of a breakthrough solid-state technology for compact and reliable high power THz sources as well as for fast and high-temperature THz detectors is highly desired.

Efficient and miniaturized quantum cascade laser (QCL) sources operating in the THz range have been developed in the last few years.[4,5] Despite the still cryogenic operating temperatures QCLs actually show high output powers and efficiencies,[5–7] a wide operating frequency range (1.2–4.5 THz),[5,8,9] spectral purity,[10] stability, and compactness, therefore becoming the more versatile radiation source across the far-infrared. However, to make the QCL technology appealing and useful for imaging and spectroscopic applications, the development of a suitable sensitive, fast, and compact detector technology is crucial to fully exploit the QCL capabilities.

Many THz detection system approaches have been developed so far, although a miniaturized room-temperature detector technology, which can be also easily integrated in an array configuration, is still largely missing. Conventionally, bolometric systems can be indeed easily coupled with QCLs[11] displaying excellent noise equivalent powers (NEP $=2\times10^{-14}$ W/Hz$^{1/2}$) and high modulation bandwidths ($\approx$1 MHz and above for superconducting elements), but at the cost of a deep cryogenic cooling and often a low dynamic range. On the other hand, high-temperature THz detectors are either not very sensitive, or extremely slow, or operate well only at frequencies lower than $\sim$1 THz, therefore being not ideal for QCL sources. Commercial micro-bolometer THz focal plane arrays[12,13] can be efficiently coupled with a QCL but presently provide only moderate sensitivities and response speed.

Fast electronic THz detectors have been realized in the last years in high-electron-mobility transistors (HEMT),[14] field effect transistors (FET),[15] and complementary metal-oxide semiconductor (CMOS)[16] architectures showing fast response times in the sub-THz range and high detectivities.[17,18] Although in principle easily scalable to even large arrays, these technologies are still limited to frequencies of few hundred GHz, above which responsivity rapidly drops. However, the responsivity can be easily maximized with the gate bias, while measuring the output at the drain with no source-drain bias applied. This significantly improves the signal-to-noise ratio. More recently, the FET detection mechanism has been exploited to develop high-detectivity, room-temperature detectors operating at 0.3 THz employing semiconductor nanowires (NWs) as active channel in a 1D configuration.[19] In the first implementation, room temperature responsivity values of $\approx$1.5 V/W and NEP $\leq 2.5\times10^{-9}$ W/Hz$^{1/2}$, already comparable with commercial thermal THz uncooled detection systems, have been obtained.[19] Here we report on the development of a one-dimensional nanowire FET THz detector operating up to 1.5 THz, efficiently coupled with a THz QCLs and showing a dramatic improvement in terms of sensitivity and modulation bandwidth.

Semiconductor nanowires represent an ideal building block for implementing rectifying diodes or plasma-wave detectors that could be well operated into the terahertz, thanks to their typical attofarad–order capacitance. As active channel of our FET detectors we select InAs nanowires since they show reasonably high electron mobility[20] even at room temperature ($\mu\approx1000$ cm^2/Vs) and a potentially long electron mean free path, enabling high transconductance at very low drive voltages.

1.5-μm-long InAs nanowires having a diameter of $\approx$30 nm were grown bottom-up on InAs (111)B substrates by chemical beam epitaxy (CBE) in a Riber Compact-21 system by Au-assisted growth using trimethylindium (TMIn) and tertiarybutylarsine (TBAs) as metal-organic (MO) precursors.[21] For n-type doping during the growth we used ditertiarybutyl selenide (DtBSe) as selenium source and fixed its line pressure at 13.3 Pa to achieve a Se doping level of $\approx10^{16}$ cm^3. Se-doping can be used to control both the charge

density and optimizing source-drain and contact resistance, while ensuring sharp pinch-off in the FET transconductance.

NWs were then mechanically transferred to a 350-μm-thick high-resistivity Si substrate with a 500 nm SiO_2 insulating surface layer. The samples were then spin-coated with e-beam sensitive resist, and contact patterns were exposed by electron beam lithography. To increase the asymmetry and therefore the responsivity of our nanowire detectors, we designed, as contact pads, low shunt-capacitance antennas to funnel the radiation into the strongly sub-wavelength detecting element. Antenna coupling ensures indeed selective responsivity to both the spatial mode and the polarization of the incoming radiation. A broad-band bow-tie (see Fig. 1(a)) dipole antenna has been therefore patterned between the source and the gate contact, with each bow-tie arm having a length of 100 μm. The gate was lithographically designed to be lateral to the nanowire at a distance of 50 nm, with no physical contact and a channel length $L = 100$ nm (see Fig. 1(b)). Surface oxides were then removed and the InAs contact areas passivated by using a highly diluted ammonium polysulfide (NH_4S_X) solution, before contact metal deposition, to prevent re-oxidation. This treatment proved to be really crucial for an optimal electrical behavior of our devices, due to the high surface-to-volume ratio of the nanowires. Ohmic contacts were then realized by thermally evaporating a Ti(10 nm)/Au(90 nm) layer onto the samples. The Si substrate was finally lapped down to 80-100 μm, and the device was mounted on a DIL package, after being preventively kept one day under vacuum.

The device electrical characterization was performed by employing the DACs of a SR830 amplifier to drive independently the source-to-drain (V_{sd}) and the gate (V_g) voltages. The drain contact was connected to a current amplifier converting the current into a voltage signal with an amplification factor of 10^4 V/A. The latter signal was then measured with an Agilent 34401 A voltmeter reader. An ohmic behavior was observed at room temperature, while sweeping V_{sd} from -0.025 to 0.025 V and while varying the gate voltage

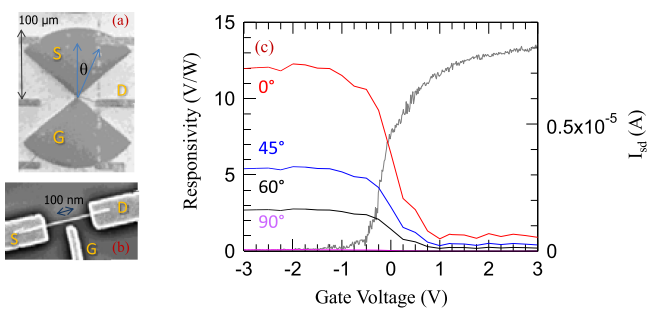

FIG. 1. (a) Scanning electron microscope (SEM) image of the detector showing the bow tie antenna patterned between the source (S) and gate (G) contacts. Each bow-tie arm was 100 μm long and featured an aperture angle of 105°. (b) SEM image of a lateral gate nanowire device. The source, drain (D) and gate contacts are marked on the picture. The source and drain pads are linked through thin connection stripes, having an almost 90° orientation angle, to one antenna lobe or to the drain main contact area, respectively. (c) Responsivity of the NW FET to the radiation of a 1.5 THz QCL, modulated at 333 Hz, as a function of the gate voltage measured at T = 300 K, and at zero applied V_{ds} while the polarization of the incoming beam is at an angle θ with respect to the bow-tie antenna axis. The left vertical axis shows the current-voltage (I_{ds}-V_g) transfer characteristic measured at room temperature and at a drain to source voltage $V_{ds} = 0.005$ V.

in the range $[-3; +3$ V]. At gate voltages $V_g > -0.5$ V, the FET channel starts to conduct and the resistance R_d reaches a $\approx 600\,\Omega$ value at current saturation; it increases instead up to about 500 kΩ in the subthreshold region, i.e., at gate voltages V_g lower than the voltage pinch off value V_t as shown from the current (I_{ds}) versus V_g characteristic, plotted in Fig. 1(c) and measured while keeping $V_{sd} = 0.005$ V.

Photoresponse experiments were performed by using a 1.5 THz QCL,[8,22] fabricated in a double-metal waveguide and operating at T = 10 K in pulsed mode, with a train of 2168 pulses (1.7 A amplitude, 435 ns pulse width, 62.8% duty cycle) repeated at a modulation frequency of 333 Hz. The QCL active region design is based on a combined bound-to-continuum and LO-photon depletion scheme.[22] The radiation was collimated and focused on the antenna by a set of two f/1 off-axis parabolic mirrors, and the photo-induced source-drain voltage was measured by using a lock-in without any pre-amplification stage. The vertically polarized incoming radiation impinges from the free space onto the nanowire devices through a $\approx$1 mm diameter pinhole with an optical power $P_t \approx 200\,\mu$W. The latter was measured with a pyroelectric detector and compared with the P_t values extracted with a calibrated absolute terahertz power meter (Thomas Keating Instruments). The detector was moved with a motorized X-Y translation stage.

The responsivity was extracted from the measured photo-induced voltage $\Delta u(V_g) = 2\sqrt{2}.\frac{\pi}{4}.LIA$ by using the relation: $R_v = (2\sqrt{2} \times \frac{\pi}{4} \times LIA \times S_t)/(P_t S_a)$, where S_t is the radiation beam spot area, S_a is the active area, and *LIA* the lock-in signal. Loading effects due to the finite impedance of the lock-in input were neglected.[19] The latter formula assumes that the entire power incident on the antenna is effectively coupled to the nanowire FET. However, owing to the relatively high nanowire impedance, it is likely that a considerable fraction of the radiation field is not properly funneled onto the device due to the impedance mismatch with the antenna output ($<100\,\Omega$), meaning that our responsivity values have to be considered as a lower limit.

In the present case, taking into account the QCL beam spot diameter $d \approx 1$ mm, $S_t = \pi d^2/4 = 0.79 \times 10^{-6}$ m^2. Moreover, since the total area of our nanowire transistor including the antenna and the contact pads was smaller than the diffraction limited area $S_\lambda = \lambda^2/4$, the active area was taken equal to S_λ. The latter area is roughly a factor of 2 larger

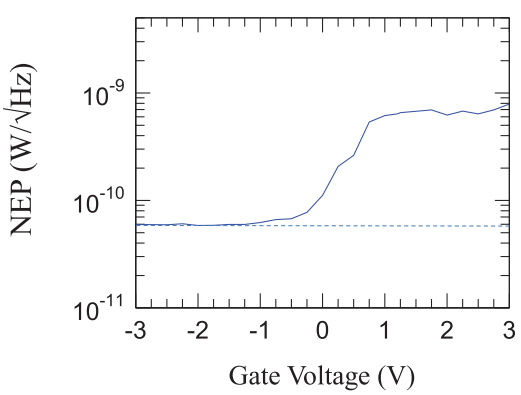

FIG. 2. Noise equivalent power as a function of the gate voltage. The dashed line shows the minimum recorded NEP value.

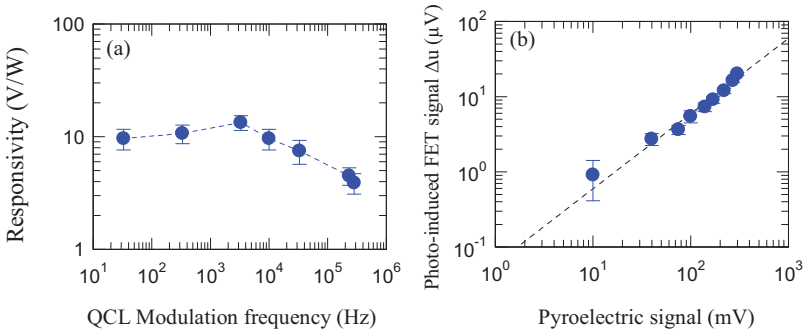

FIG. 3. (a) Detector responsivity plotted as a function of the QCL modulation frequency. The dashed line is a guide to the eye. (b) Photoresponse signal Δu recorded while varying the bias/current of the QCL modulated at 333 Hz, plotted as a function of the corresponding pyroelectric response. The dashed line is a linear fit to the data.

than the maximum effective area of a dipole antenna as reported in the conventional antenna theory,[23] therefore making our responsivity values an underestimation.

Figure 1(c) shows the responsivity (R_v) plotted as a function of the gate voltage V_g by varying the antenna orientation angle (θ) with respect to the polarization of the incoming beam. The detector responsivity reaches up to 12 V/W for $\theta = 0$, allowing a significant improvement of our detector performances with respect to previous experimental reports at 0.3 THz,[19] despite the 5 times higher operating frequency. This is mostly due to three main factors: (i) the one order of magnitude reduction of the NW resistance; (ii) the antenna geometry perfectly resonant with the 1.5 THz QCL; (iii) the narrow gates employed.[20] It is worth noticing that while θ increases, the detector responsivity is drastically reduced by more than one order of magnitude, confirming the efficiency of the employed antenna geometry.

Figure 2 shows the NEP as a function of the gate voltage, measured from the ratio N/R_v, where N is the transistor noise that we can assume almost equal to the Johnson–Nyquist one $N = \sqrt{4kTR}$ as confirmed by previous experimental reports.[19] A minimum NEP value of $\sim 6 \times 10^{-11}$ W/$\sqrt{}$Hz is reached in the sub-threshold regime, confirming the dramatic improvement of our detector sensitivity levels, significantly better than commercial thermal uncooled detection system operating at frequencies $\sim$1 THz.[24]

To test the response times of our NW detectors we modulated the QCL beam in a frequency range spanning from 33 Hz up to ≈300 kHz. The detector responsivity as a function of the modulation frequency is displayed in Fig. 3(a). Within a four decades bandwidth R_v decreases by a factor of 3, still remaining significantly higher than 1 V/W, meaning that the response speed of our room temperature detectors is really competitive with any cooled detection systems operating in the far-infrared. It is worth noticing that the employed experimental set-up poses a limit on the maximum modulation frequency at ≈300 kHz. The corresponding response time (≈3μs) has then to be considered as an upper limit.

Finally, to investigate the dynamic range of our devices we checked their linearity against the standard THz pyroelectric system. Figure 3(b) shows the nanowire FET photo-induced voltage Δu measured while varying the QCL drive current in its operating regime and by simultaneously recording the QCL optical power with a pyroelectric detector while the modulation frequency is fixed at 333 Hz. The trend is basically linear, up to the highest QCL power.

This work was partly supported by the Italian Ministry of Education, University, and Research (MIUR) through the program "FIRB-Futuro in Ricerca 2010" RBFR10LULP "Fundamental research on terahertz photonic devices" and by the "Terasuper" project of the Italian Ministry of Defense. The authors would like to thank M. Fischer for the growth of the QC heterostructure and C. Walther for the processing of the QC laser.

[1]M. Tonouchi, Nat. Photonics **1**, 97 (2007).
[2]H. W. Hubers, S. G. Pavlov, H. Richter, A. D. Semenov, L. Mahler, A. Tredicucci, H. E. Beere, D. A. Ritchie, Appl. Phys. Lett. **86**, 244104 (2005).
[3]P. Shumyatsky and R. R. Alfano, J. Biomed. Opt. **16**, 033001 (2011).
[4]R. Köhler, A. Tredicucci, F. Beltram, H. E. Beere, E. H. Linfield, A. G. Davies, D. A. Ritchie, R. C. Iotti, and F. Rossi, Nature **417**, 156 (2002).
[5]B. S. Williams, Nat. Photonics **1**, 517 (2007).
[6]M. S. Vitiello, G. Scamarcio, J. Faist, G. Scalari, C. Walther, H. E. Beere, and D. A. Ritchie, Appl. Phys. Lett. **94**, 021115 (2009).
[7]L. Mahler and A. Tredicucci, Laser Photonics Rev. **5**, 647 (2011).
[8]G. Scalari, C. Walther, M. Fischer, R. Terazzi, H. E. Beere, D. Ritchie, and J. Faist, Laser Photonics Rev. **3**, 45 (2009).
[9]M. S. Vitiello and A. Tredicucci, IEEE Trans. terahertz Sci. Technol. **1**, 76 (2011).
[10]M. S. Vitiello, L. Consolino, S. Bartalini, A. Taschin, A. Tredicucci, M. Inguscio, and P. D. Natale, "Quantum-limited frequency fluctuations in a Terahertz laser," Nature Photonics (in press).
[11]S. Cibella, M. Ortolani, R. Leoni, G. Torrioli, L. Mahler, J. H. Xu, A. Tredicucci, H. E. Beere, and D. A. Ritchie, Appl. Phys. Lett. **95**, 213501 (2009).
[12]B. N. Behnken, G. Karunasiri, D. R. Chamberlin, P. R. Robrish, and J. Faist, Opt. Lett. **33**, 440 (2008).
[13]A. W. M. Lee, Q. Qin, S. Kumar, B. S. Williams, Q. Hu, Appl. Phys. Lett. **89**, 141125 (2006).
[14]A. M. Hashim, S. Kasai, and H. Hasegawa, Superlattice Microstruct. **44**, 754 (2008).
[15]W. Knap, F. Teppe, Y. Meziani, N. Dyakonova, J. Lusakowski, F. Boeuf, T. Skotnicki, D. Maude, S. Rumyantsev, and M. S. Shur, Appl. Phys. Lett. **85**, 675 (2002).
[16]Y. M. Meziani, J. Lusakowski, N. Dyakonova, W. Knap, D. Seliuta, E. Sirmulis, J. Deverson, G. Valusis, F. Boeuf, and T. Skotnicki, IEICE Trans. Electron. **E89-C**, 993 (2006).
[17]F. Schuster, D. Coquillat, H. Videlier, M. Sakowicz, F. Teppe, L. Dussopt, B. Giffard, T. Skotnicki, and W. Knap, Opt. Express **19**, 7827 (2011).
[18]S. Boppel, A. Lisauskas, V. Krozer, H. G. Roskos, Electron. Lett. **47**, 661 (2011).
[19]M. S. Vitiello, D. Coquillat, L. Viti, D. Ercolani, F. Teppe, A. Pitanti, F. Beltram, L. Sorba, W. Knap, and A. Tredicucci, Nano Lett. **12**, 96 (2012).
[20]L. Viti, M. S. Vitiello, D. Ercolani, L. Sorba, and A. Tredicucci, Nanoscale Res. Lett. **7**, 159 (2012).
[21]D. Ercolani, F. Rossi, A. Li, S. Roddaro, V. Grillo, G. Salviati, F. Beltram, and L. Sorba, Nanotechnology **20**, 505605 (2009).
[22]C. Walther, M. Fischer, G. Scalari, R. Terazzi, N. Hoyler, and J. Faist, Appl. Phys. Lett. **91**, 131122 (2007).
[23]C. A. Balanis, *Antenna Theory* (Wiley, Hoboken, New Jersey, 2005).
[24]F. Sizov and A. Rogalski, Prog. Quantum Electron. **34**, 278 (2010).